



Universidad Politécnica de Cartagena
Departamento de Tecnologías de la Información y las Comunicaciones

Máster Universitario en Ingeniería de Telecomunicación

Reutilización Eficiente del Espectro en Redes Celulares mediante Optimización Estocástica

José Antonio Ayala Romero

Director:

Juan José Alcaraz Espín

Marzo 2015

Autor: José Antonio Ayala Romero

E-mail del autor: jayalaromero@gmail.com

Director: Juan José Alcaraz Espín

E-mail del director: juan.alcaraz@upct.es

Título: Reutilización Eficiente del Espectro en Redes Celulares mediante Optimización Estocástica

Title: Efficient Spectrum Reuse in Cellular Networks with Stochastic Optimization

Descriptores: Spectrum reuse, cognitive radio, cellular systems, interference management

Titulación: Máster Universitario en Ingeniería de Telecomunicación

Departamento: Tecnologías de la Información y las Comunicaciones

Fecha de presentación: Marzo 2015

Resumen

Aproximadamente cada diez años, una nueva tecnología celular es desarrollada y puesta en el mercado. Sin embargo, los operadores se ven obligados a mantener sus redes antiguas debido a que no todos los usuarios migran a nuevas redes a la vez. Por tanto, el espectro asociado a esas redes antiguas cada vez está más infrautilizado. Usando técnicas de radio cognitiva, el operador puede permitir a los usuarios de las redes más nuevas reutilizar ese espectro. Se propone un esquema de acceso semi-distribuido donde el operador guía al usuario secundario difundiendo algunos parámetros operacionales de la estrategia de acceso. Este mecanismo aprende de forma dinámica los parámetros óptimos por medio del algoritmo Response Surface Methodology (RSM), que requiere muy poca señalización. Los resultados muestran un notable aumento de la capacidad comparado con los clásicos esquemas de uso de oportunidades temporales o espaciales.

Abstract

As cellular network technology evolves, the operators deploy new generation networks while maintaining their legacy networks, since not all users upgrade their terminals at the same pace. Therefore, the spectrum associated to these legacy networks becomes gradually underused. By means of cognitive radio techniques, the operator can allow its new generation terminals to reuse this spectrum. We propose a semi-decentralized scheme in which the operator guides the secondary access by broadcasting some operational parameters of the access strategy. The mechanism dynamically learns the optimal parameters by means of a response surface methodology (RSM), implying a very small signaling overhead. Our results show a notable capacity improvement compared to the classical approaches of exploiting spatial or temporal opportunities.

Contents

| | | |
|----------|--|-----------|
| 1 | Introduction | 1 |
| 1.1 | Interference Management Techniques | 1 |
| 1.2 | Scenario Description | 3 |
| 1.3 | Content Structure | 3 |
| 2 | Related Work | 4 |
| 3 | Exploiting Temporal and Spacial Opportunities | 5 |
| 3.1 | Introduction | 5 |
| 3.2 | System Description | 5 |
| 3.2.1 | Secondary Access over Temporal Opportunities | 6 |
| 3.2.2 | Secondary Access over Spatial Opportunities: Dual Tessellation | 6 |
| 3.3 | Hybrid Access | 8 |
| 3.3.1 | Formulation of the Design Problem | 8 |
| 3.4 | Numerical Results | 10 |
| 3.4.1 | Evaluation Framework | 10 |
| 3.4.2 | Performance Results | 11 |
| 3.5 | Conclusions | 12 |
| 4 | Stochastic Optimization Approach: The Unconstrained Case | 14 |
| 4.1 | Introduction | 14 |
| 4.2 | System description | 15 |
| 4.3 | Problem Formulation | 17 |
| 4.4 | Response Surface Method (RSM) Algorithm | 18 |
| 4.4.1 | Algorithm Formulation | 18 |

| | | |
|----------|---|-----------|
| 4.4.2 | System Operation | 20 |
| 4.5 | Numerical Results | 21 |
| 4.5.1 | Evaluation Framework | 21 |
| 4.5.2 | Convergence and Usage of the Frequency Bands | 21 |
| 4.5.3 | Effect of the Traffic Intensity | 23 |
| 4.6 | Conclusion | 25 |
| 5 | Stochastic Constraints for Primary Transmission Protection | 26 |
| 5.1 | Introduction | 26 |
| 5.2 | System description | 26 |
| 5.3 | Response Surface Method (RSM) Algorithm with Stochastic Constraints | 27 |
| 5.3.1 | Algorithm Formulation | 27 |
| 5.3.2 | Algorithm Operation | 29 |
| 5.3.3 | Sampling and Update of the ρ Vector | 30 |
| 5.4 | Daily Traffic Application | 30 |
| 5.5 | Conclusion | 32 |
| 6 | Conclusion | 33 |

Chapter 1

Introduction

Approximately every decade, a new cellular access technology is developed and introduced in the market. However, because not all users upgrade their terminals at the same pace, the operators have to keep their legacy networks working, and the radioelectric spectrum assigned to these old networks becomes gradually more and more underused. On the other hand, the emerging technologies have increasing spectrum necessities due to the bandwidth demanded by the new applications.

In this work we address this issue by exploiting cognitive radio techniques [11]. The terminals of the newest network would be the secondary users (SUs), and the terminals of the legacy network would be the primary users (PUs). The secondary users are allowed to opportunistically access the underused spectrum of the primary network.

One of the most critical issues in this type of solution is the potential interference between nearby secondary users and from secondary users to primary users. This issue harms the overall system capacity and therefore must be addressed. In the next section we describe some general techniques of interference and resource management.

1.1 Interference Management Techniques

The different techniques to reduce the interference and increase the capacity and performance can be classified according to different criteria such as system versus user-centric approaches, centralized versus distributed control strategies and so on [3]. Then, we present below a classification of interference management techniques.

The *system-centric* approaches propose a mathematical model to optimize the system QoS parameters such as transmission power and total data rate. In this approach, the overall performance of the total system is more important than the performance of individual user. Thus, the fairness between users is difficult to be guaranteed.

However, *user-centric* approaches can guarantee the fairness between users because they try to optimize a utility function that represents application requirements, that is, the service satisfaction of each user. Hence, excessive allocation of resources is prevented by allocating the

appropriate amount of resource to each user. The aim of the user-centric approach is to maximize the average utility of the system.

Hardware approaches consist of applying MAC or physical techniques to mitigate or control interference by means of multi-antenna techniques, MIMO systems, etc.

Regarding the *resource allocation*, it can be classified as static, where the resource allocation remains fixed over time or dynamic, where the allocation changes in adapt to the load variations.

There are two schemes that can be used for dynamic partition: centralized or distributed. In a centralized approach, the resources are assigned to the primary users and secondary users by means of a central controller. This approach achieves more efficient resource utilization, however the signaling overhead is higher and more complex. On the other hand, the distributed control avoids the bottleneck effect of a centralized control entity but the overall performance is lower.

Due to the enormous number of secondary users that can be expected, the computational complexity of the previous approaches is a challenging issue. Hence, using a cognitive approach the resource management scheme shall be able to utilize the radio resources not occupied by the primary network autonomously. Thus, the device has the ability to collect information from its surrounding environment in order to allow the equipment to adapt its behavior to the local context properly. We can classify the cognitive radio approaches as follow:

- *Interweave approach*: Secondary users can passively look for unused frequencies for opportunistic access. This approach restricts the system capacity since there is no spatial reuse.
- *Underlay approach*: This approach exploits spatial reuse in a intensive manner as long as the resulting aggregated interference at primary receivers is lower than the outage constraint. However, without information of the location, the secondary users are unable to distinguish whether the occupied frequency band are assigned to a primary network in its vicinity or not. Therefore, the worst case is assumed.
- *Controlled underlay approach*: In this approach the secondary users have location information, consequently they are able to determine the set of frequency bands that can be reused without causing (to primary user in their vicinity) harmful interference.

Sometimes, when we assume that the secondary users are non-cooperative, that is, there is no mutual communication/coordination, *Q-learning schemes* like Reinforcement-Learning (RL), can be applied. In this approach secondary users need to self-organize by learning from their environment (by trials and errors), and adapt their strategy until reaching convergence.

Finally, *the access control scheme* plays an important role in interfere avoiding. We define the interference temperature as the secondary aggregated interference. The aim of this scheme is to keep the interference temperature under an acceptable level.

1.2 Scenario Description

Motivated by the problem of spectrum scarcity in new generation networks and the underutilized spectrum of the legacy networks, we allow the users of the newest networks to opportunistically access the spectrum of the legacy networks to increase the spectrum efficiency.

The secondary access to the spectrum of the primary (legacy) network should not cause noticeable degradation to PU transmissions. In this scenario, the operator owns and control both the primary and the secondary networks, and therefore can establish the rules for secondary access and monitor the impact of these rules on the performance of both SU and PU transmissions. However, we assume no modifications on the legacy network, implying that the operation of the secondary network is transparent to the primary network.

We consider that the SUs establish point-to-point connections among them (cognitive pairs) in an ad-hoc fashion. We propose a semi-decentralized secondary access scheme allowing each SU to access a set of primary frequency bands using either temporal or spatial spectrum holes (opportunities). By giving more access options to each SU, this approach can outperform previous, more limited, mechanisms. To fully exploit its potential, we describe an on-line algorithm that, with very small computational and signaling overhead, allows the system to learn the optimal SU access policy in terms of capacity.

1.3 Content Structure

Chapter 2: Related Work. Review of state-of-art where we compare this work with other similar works.

Chapter 3: Exploiting Temporal and Spacial Opportunities. We propose a hybrid access scheme to exploit either spatial and temporal opportunities to improve the SU capacity keeping the PU performance above of a minimum threshold.

Chapter 4: Stochastic Optimization Approach: The Unconstrained Case. We propose a semi-decentralized secondary access scheme where all spectrum of the system is available to each SU. In addition, the system is capable of learning the optimal frequency distribution of the SUs using Response Surface Methodology algorithm.

Chapter 5: Stochastic Constraints for Primary Transmission Protection. In this chapter, we reformulate the algorithm adding stochastic restrictions allowing the system to find the optimum parameters taking into account the minimum PU performance required.

Chapter 6: Conclusion We present the final conclusion of this work.

Chapter 2

Related Work

Previous works have proposed the combination of temporal and spatial sensing by the SUs [4], [5], [6], [7]. Works like [4] and [5] consider a single secondary transmitter and exploit information from spatial sensing to improve the performance of temporal sensing. The single transmitter model is also applied in [6] for vehicular networks. In [7] the capacity is optimized by randomizing the access strategies, but for a single PU, single SU scenario. However, the motivational scenario of our work comprises multiple secondary transmitters with multiple primary base stations. Thus, we must consider relevant features that are not captured by the single transmitter model, such as the inter SU-interference and the frequency reuse in a cellular structure.

In cellular networks, previous works as [8] and [9] have addressed spatial spectrum reuse by a secondary network. However, these works assume that the secondary users only scan one frequency. As pointed out by their authors, scanning all the frequencies would improve the performance. In chapter 3 we follow this suggested approach and present an access scheme where each SU can exploit spatial and temporal opportunities. Each SU is allowed to access two frequency bands, selecting one of them randomly according to a probability distribution provided by a central controller.

In the following chapters, we present a semi-distributed mechanism for opportunistic spectrum access in which all the spectrum of the system can be made available to each SU. The main contributions are the following: 1) Each SU can exploit spatial and temporal opportunities over a larger amount of bandwidth, resulting in higher SU capacity. 2) The system is evaluated in a realistic setting considering irregular cell shapes. 3) And, the most important feature, the system is capable of learning the optimal probability distribution over the frequency bands of the cellular network.

The learning algorithm applies the response surface methodology (RSM) [12], whose application is novel in interference management problems. Finally, applying the response surface methodology with stochastic restrictions algorithm [13] we assure the coexistence of both primary and secondary networks.

Chapter 3

Exploiting Temporal and Spatial Opportunities

3.1 Introduction

In this chapter, we propose a secondary hybrid access scheme to exploit either spatial and temporal opportunities. The aim of this access is to improve the SU capacity while the PU performance is above the minimum required value.

In the scenario we propose, we consider that the SUs establish point-to-point connections among them (cognitive pairs) in an ad-hoc fashion. This ad-hoc network enables multiple applications such as relying devices to increase 4G indoor coverage, device-to-device communications, or increasing the bandwidth of a small cell providing offloading services.

Typically, secondary spectrum access is based on occupying either temporal or spatial spectrum holes (opportunities). Our proposal consists on exploiting both strategies simultaneously, combining them into an hybrid access scheme.

The contribution of this chapter is to develop and evaluate a new hybrid secondary access scheme combining access over temporal and spatial opportunities. An improvement with respect to previous works is that our method is especially conceived for cellular networks, considering multiple PU transmitters within a cell structure. We also introduce the new concept of *dual tessellation*, which characterizes the spatial opportunities in cellular scenarios with frequency reuse. Next section describes the system and the basic secondary access schemes. The hybrid scheme is discussed in Section 3.3 and evaluated in Section 3.4.

3.2 System Description

The system considered comprises two overlay networks: a legacy cellular network (primary network) and a secondary ad-hoc network. The primary network contains primary base stations (PBSs) and terminals, also referred to as primary users (PUs). Each PBS provides coverage to

a certain geographical area (primary cell) and uses a frequency band different from its adjacent cells. Dividing all the covered region into cells (tessellation) increases the capacity of the wireless access network. In this chapter we consider hexagonal cells and a frequency reuse scheme using 7 frequency bands (reuse factor 7). We refer to a cell using band f_i as an f_i -primary cell. Nevertheless, our framework is applicable to any tessellation and frequency reuse scheme. Each frequency band is divided into $2N$ orthogonal channels (N downlink and N uplink channels). Time is divided into time-slots and the data transmitted over a single PU channel in a time-slot is referred to as *packet*. Next subsections explain the two strategies for SU spectrum access that we later combine into our hybrid access approach.

3.2.1 Secondary Access over Temporal Opportunities

Let us consider an f_i -primary cell, \mathcal{A}_i , using a spectrum band f_i with N uplink channels and N downlink channels. Because SUs only sense and access downlink channels, we consider that *PU activity* on a channel refers to data transmission from the PBS to a PU over this channel. Depending on the PU traffic intensity, some channels are free of data transmission during some periods of time. A period free of PU activity on a given channel is referred to as a *temporal opportunity*. A secondary transmitter located in \mathcal{A}_i can simultaneously occupy up to m channels within f_i if it detects a temporal opportunity on each of these channels.

This spectrum reuse strategy typically implies two consecutive phases: scanning and transmission. The scanning phase allows the cognitive pair to detect PU activity and find temporal opportunities on f_i . When one or more available channels are found, the cognitive pair starts the transmission phase over these channels. If PU activity is detected in any of the occupied channels, the SU transmission on this channel is switched off. The detection of PU activity during the SU transmission phase can be done in several ways [11]: some of them rely on periodically switching off transmission and listening the channel, while others assume that the SU receiver can detect transmission overlap. We use the latter one. In particular, we consider that the overlap is detected by means of a maximum a posteriori (MAP) estimator.

Note that, even with such a detection mechanism, transmission overlap occurs in some time-slots. In a time-slot with collision, the SINR at the PU receiver decreases, sometimes causing the incorrect reception of the packet transmitted in that time-slot.

The SU access is intended to be *transparent* to the primary network, in the sense that it does not require the adoption of any specific signaling at the primary network devices, and the performance of PU communications should not be noticeably reduced by SU activity.

3.2.2 Secondary Access over Spatial Opportunities: Dual Tessellation

Using spatial opportunities implies that the channels of frequency band f_i can only be used by the SUs outside the f_i -primary cells. The drawback is that the SUs cannot detect PU activity on the f_i channels, but, if the SUs are sufficiently distant from the primary cell, the co-channel interference at the PU terminals remains at an acceptable level. We define the f_i -dual cells as the

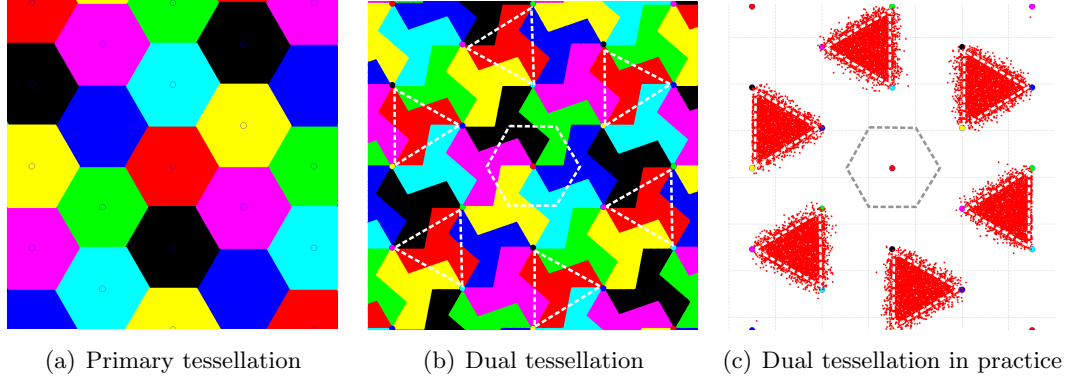


Figure 3.1: Example of the dual tessellation for a hexagonal cell structure with reuse factor 7. Each color corresponds to one frequency band.

geographical areas where an SU transmitting over the f_i band causes less average interference on the closest f_i -primary cell than the interference it would cause on any f_j -primary cell ($j \neq i$) when transmitting over f_j . These f_i -dual cells are the spatial opportunities of our model. The location of an SU is therefore associated to an f_i -primary cell, \mathcal{A}_i , and an f_j -dual cell, \mathcal{D}_j , such that $f_i \neq f_j$.

By transmitting over dual cells, the secondary network is determining an overlay cell structure that we refer to as the *dual tessellation*, which has the same frequency reuse factor of the primary network, and enhances the capacity of the secondary network as well.

Example. Let us consider a primary network using an hexagonal cell structure with reuse factor 7. Figure 3.1(a) shows a hexagonal tessellation where each cell is assigned one of the 7 frequency bands. This is the classic theoretical cell structure assuming a regular PBS location pattern and considering only distance attenuation. Figure 3.1(b) shows the corresponding dual tessellation, highlighting the dual cells of the primary cell located at the center of the figure. As we can see, each dual cell can be approximated by a triangle whose vertices coincide with the location of 3 PBSs. The frequencies of these 3 PBSs determine the frequency of the dual cell. In practice, before using a spatial opportunity, an SU needs to detect the frequencies of the surrounding PBS in order to determine to which dual cell it belongs. One way to do this is to take samples of the pilot tones at each f_i . The 3 frequencies with the highest estimated average power for the pilot tone are considered the frequencies of the closest PBSs. This process can be subject to estimation errors. Figure 3.1(c) shows the dual cells obtained for a single f_i with the imperfect sampling scheme described in Section 3.4. Note that because this scheme is based on average power detection, it is also applicable to the general case of irregular cell shapes.

The PUs in an f_i -primary cell will receive co-channel interference from the PBSs of other f_i -primary cells and from the SUs located at f_i -dual cells. Regarding the interference caused by the SU network, the following considerations should be highlighted. Because of its ad-hoc nature, the power of an SU transmission on each channel can be very small compared to a PBS transmission. More importantly, while the typical location of a PBS (outdoors and on top of a relatively high building) is intended to provide coverage to a wide area, a secondary transmitter is usually a user terminal, and its location (indoors or outdoors at small heights) will cause the

SU signal power to decrease faster with distance compared to the transmission of a PBS. As a consequence, although the f_i -dual cells are closer to the f_i -primary cell than other f_i -primary cells, the interference at the PUs can still be below the required objective.

3.3 Hybrid Access

When SUs exploit temporal or spatial opportunities, they are in fact adopting the primary or the dual tessellation respectively. However, the capacity of each cell (primary or dual) is limited for secondary users as well, because of the intra and inter cell interference, and the limitation in the number of available channels when using temporal opportunities.

One way to increase the capacity for the secondary network is to simultaneously use the primary and the dual tessellation, therefore duplicating the area where each frequency band can be used by the secondary terminals. This approach is the **hybrid access** and comprises the following 3 steps:

1. Before transmitting, an SU randomly selects one type of secondary access: with probability ρ it will look for a temporal opportunity and with probability $1 - \rho$ it will exploit spatial opportunities.
2. If the SU selects to access over temporal opportunities, it will proceed as described in Subsection 3.2.1 to transmit over channels of the f_i -primary cell where the SU is in.
3. If the SU selects to access over spatial opportunities, it will detect the dual cell D_j where the SU is in, and will transmit over f_j channels as described in Subsection 3.2.2 (recall that $f_j \neq f_i$).

Note that ρ determines the proportion of secondary terminals using each type of access. The interference from SUs using temporal opportunities will be very intense (intra cell interference), but will be seldom and will last short periods of time (depending on the accuracy of the PU activity detection). On the other hand, the interference from the SUs on dual cells will be sustained over time, but will be less intense (similar to the co-channel interference from other PBSs). To properly design the hybrid access we should combine the effects of these two types of interference into a single performance metric for the primary terminals: the probability of correct reception per time-slot. In the scenario considered, it is the operator owning both the legacy and the secondary networks who can determine, and broadcast to the SUs, the proper value of ρ such that the PU performance remains acceptable and the SU capacity is maximized.

3.3.1 Formulation of the Design Problem

In this subsection we define the performance metrics for both the primary and secondary terminals and formulate the problem that the operator needs to solve to determine ρ .

Let Γ_t^{PU} be the SINR at a given downlink channel, in time slot t , measured at a PU receiver. We will assume that the PU receiver is placed on the worst-case location in terms of interference

from the secondary transmitters. Moreover, we only consider samples where there is an active PU transmission on the channel ($\Gamma_t^{PU} > 0$, for $t = 1, 2, \dots$). The amount of interfering SUs and their locations change randomly over time. Let N_t^{SU} denote the number of SU transmitters using the channel (and the frequency band f_i) of the PU receiver, at time-slot t . Moreover, for a given SU location, the interference power changes over time because of fading effects. Let $I_t(n)$ denote the interference power received from the n -th SU interferer at time-slot t . We have that

$$\Gamma_t^{PU} = \frac{P_{Rx,t}^{PU}}{N_0 + I^{PU} + \sum_{n=1}^{N_t^{SU}} I_t(n)} \quad (3.1)$$

where $P_{Rx,t}^{PU}$ is the signal power at time-slot t , N_0 is the thermal noise and I^{PU} is the aggregated interference from PBSs using f_i . Note that Γ_t^{PU} is a discrete-time stochastic process. The probability of correct reception at the PU receiver, P_c , is given by

$$P_c = \lim_{T \rightarrow \infty} \frac{1}{T} \sum_{t=1}^T \Phi \{ \Gamma_t^{PU} > \gamma \} \quad (3.2)$$

where γ is the SINR detection threshold at the PU, and $\Phi \{z\}$ is an indicator function which equals 1 if condition z holds, and equals 0 otherwise.

When an SU accesses the spectrum, it uses up to m contiguous channels of the selected f_i band, and transmits during a random number, T_{SU} , of time-slots. Each SU transmission can be represented by m stochastic processes $\Gamma_{t,j}^{SU}$ for $j = 1, \dots, m$, such that $\Gamma_{t,j}^{SU}$ represents the SINR for channel j at time-slot t measured at a SU receiver. When using temporal opportunities, the number of channels used by the SU can change at each time slot. Obviously $\Gamma_{t,j}^{SU} = 0$ if channel j is not used, and $\Gamma_{t,j}^{SU} = 0$ for $j = 1, \dots, m$ if $t > T_{SU}$. Let C_{\max}^S be the achievable SU capacity in absence of interference, over m channels. The normalized capacity for an SU transmission can be computed as follows

$$C_s = E \left\{ \frac{1}{T_{SU}} \sum_{t=1}^{T_{SU}} \sum_{j=1}^m W \log_2 (1 + \Gamma_{t,j}^{SU}) / C_{\max}^S \right\} \quad (3.3)$$

Where the expectation is taken over T_{SU} and $\Gamma_{t,j}^{SU}$ for $j = 1, \dots, m$. The probability of selecting a temporal opportunity, ρ , determines the evolution of the stochastic processes involved in the computation of P_c and C_s . Therefore, for a given ρ , we can express these performance metrics as $P_c(\rho)$ and $C_s(\rho)$. The design objective for the hybrid access scheme is to select ρ such that $C_s(\rho)$ is maximized while $P_c(\rho)$ is above the minimum required value $\underline{P_c}$. This can be expressed as an optimization problem:

$$\max_{\rho} C_s(\rho), \text{ subject to } P_c(\rho) \geq \underline{P_c}, 0 \leq \rho \leq 1. \quad (3.4)$$

Note that, in general, we cannot expect the maximum of $C_s(\rho)$ be at $\rho = 0$ or at $\rho = 1$, since these two values minimize the area where the secondary users can use each f_i . Next section shows that, in most cases, there is an optimum between these two ρ values, which motivates the problem.

Finding the optimum ρ is a challenging task because the stochastic processes $\Gamma_{t,j}^{SU}$ and Γ_t^{PU} capture the interaction of a random number of randomly located terminals with fading effects among each pair of them. Moreover, $\Gamma_{t,j}^{SU}$ and Γ_t^{PU} take values from continuous state spaces, and therefore Markovian techniques cannot be applied. We need to resort to a Monte-Carlo approach that we explain in the following section.

3.4 Numerical Results

3.4.1 Evaluation Framework

This subsection describes the Monte-Carlo methodology and the scenario used to evaluate P_c and C_s . The primary network uses the hexagonal cell structure with reuse factor 7 described in Subsection 3.2.2. We consider pathloss and multipath fading. To compute the pathloss attenuation over distance, $A(d)$ (dB), we use the following piecewise dual-slope model [10]:

$$A(d) = \begin{cases} K + 10\gamma_1 \log_{10}(d/d_0) & d_0 \leq d \leq d_c \\ K + 10\gamma_1 \log_{10}(d_c/d) + 10\gamma_2 \log_{10}(d/d_c) & d > d_c \end{cases} \quad (3.5)$$

The parameters γ_1 , γ_2 , K and d_c are typically obtained via regression fit of empirical data. A relevant aspect is that the critical distance for SU transmissions is notably smaller than the critical distance for PBS transmissions, because the PBSs are located at high outdoor locations while SUs are located either indoors or on the ground. All the signals experience Rayleigh fading.

Primary cells have a radius $R = 700$ m. The area used to generate random terminal locations is a $6R \times 4\sqrt{3}R$ rectangle. We focus on the downlink channels of one frequency band f_i . The traffic intensities of the primary and secondary networks are determined by the arrival probabilities per time-slot. At each f_i primary cell, there can be one PU arrival per time-slot, and each active PU can departure with probability 0.1. Regarding SU transmissions, the number of new cognitive pairs at each time slot is generated by a binomial distribution characterized by 20 trials of p_{SU} probability each. Each secondary transmitter can be at any point of the whole simulated area. The probability of an SU departure at each time-slot, is 0.05. According to the ad-hoc nature of the secondary network, the secondary link distance (90 m) is notably shorter than R . However, because of co-channel interference among SUs, only up to 3 simultaneous SU transmissions can take place over the same channel in the same (primary or dual) cell.

With probability ρ , an incoming secondary transmitter will look for a temporal opportunity. Before starting transmission, the probability of correctly detecting PU activity on each channel is 0.9. During transmission, the probability of overlap detection is 0.8. With probability $1 - \rho$, the incoming SU will look for a spatial opportunity. It will then scan the pilot tones at the 7 frequency bands, taking 7 power samples of each one. For each f_i , the samples are averaged if 2 or more are received above the sensibility threshold (-80 dBm). The 3 highest average powers are considered to correspond to the 3 closest PBSs, determining the dual cell. Table 3.1

| Parameter | Assigned value |
|--|----------------|
| Primary transmitters | |
| number of downlink channels, N | 10 |
| channel bandwidth, W | 200 KHz |
| cell radius, R | 700 m |
| average received power at PU | -78 dBm |
| SINR detection threshold at PU, γ | -17 dB |
| baseline noise at PU ($N_0 + I_{PU}$) | -110 dBm |
| pilot tone transmission power | 12 W |
| Secondary transmitters | |
| average SU Tx power per channel | 0.5 W |
| SU link distance, | 90 m |
| SU multichannel limit, m | 3 |
| probability of PU activity detection | 0.9 |
| probability of overlap detection | 0.8 |
| power threshold for f_i detection, | -80 dBm |
| number of samples for f_i detection, | 7 |
| Propagation parameters | |
| pathloss exponents, γ_1, γ_2 | 2.4, 4.2 |
| propagation factor K | 46.7 dB |
| critical distance for PBS transmission | $1.2R$ m |
| critical distance for SU transmission | 100 m |

Table 3.1: Parameter setting of the reference scenario used in numerical evaluations

summarizes the simulation parameters.

To estimate P_c , we take samples of the SINR process, Γ_t^{PU} at two possible PU locations, the edge and the center of the primary cell. At each time-slot, only the lowest one is used to generate a P_c sample. The estimation \hat{P}_c is simply the arithmetic mean of the samples. To estimate C_s we need to estimate separately the capacity of the SUs using temporal holes C_s^T and the capacity of the SUs using spatial holes C_s^S . The estimations, \hat{C}_s^T and \hat{C}_s^S , are weighted to obtain the final estimation $\hat{C}_s = \rho \hat{C}_s^T + (1 - \rho) \hat{C}_s^S$.

3.4.2 Performance Results

It is clear that the traffic intensity in both the primary and secondary networks will have a notable impact on the performance metrics P_c and C_s , because it determines the amount of temporal opportunities in the primary cells, and the number of potential interfering nodes. It is therefore interesting to evaluate how this intensity affects the design of the hybrid access strategy (optimal ρ).

For a given p_{SU} , we consider different primary traffic intensities. We measure these intensities as the average number of f_i channels occupied by PUs, which is referred to as *PU occupation* and is given in percentage. Figure 3.2 shows P_c and C_s versus ρ for $p_{SU} = 0.1$ and different PU occupations ranging from 5% to 50%.

The results show that, in our scenario, the PU performance, P_c , decreases when the SUs use

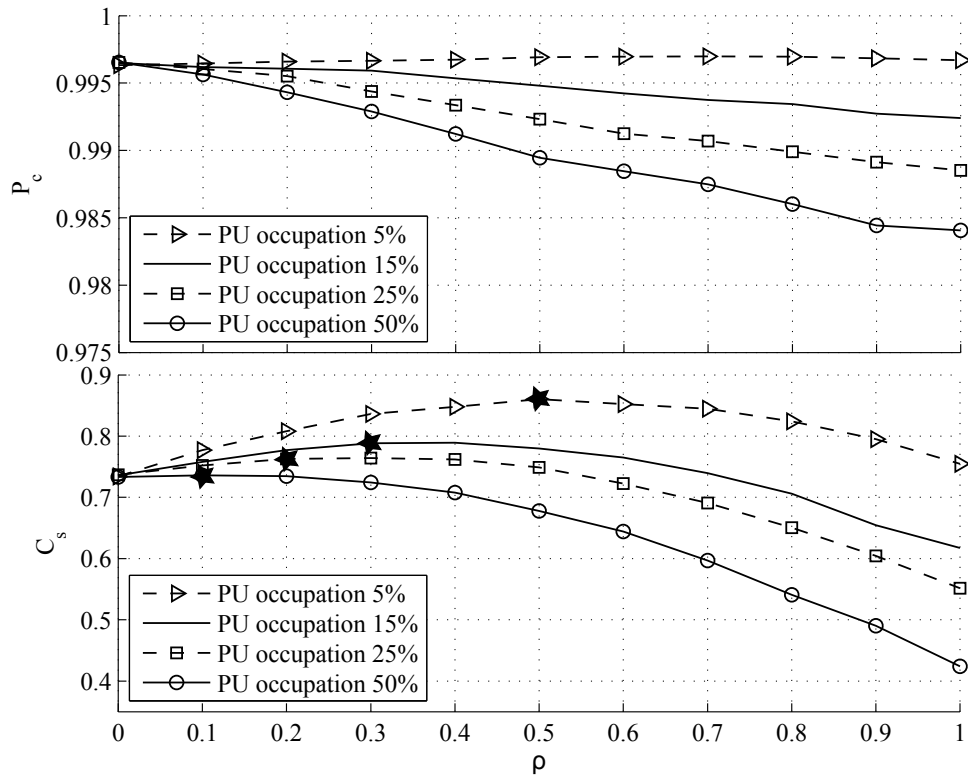


Figure 3.2: PU and SU performance versus ρ under different PU traffic intensities, for $p_{SU} = 0.1$. The stars indicate the optimum SU capacity for each PU occupation.

temporal opportunities with higher probability (higher ρ). However, as predicted, $C_s(\rho)$ attains its optimum value for a ρ within the open set $(0, 1)$. The optimal ρ is closer to 0 at higher values of PU occupation for two reasons: first, when the PU traffic is higher there will be less temporal opportunities and, second, the SU terminals using temporal opportunities will experience more transmission overlap, which also reduces their capacity.

Let us see the effect of a higher SU traffic by duplicating it. Figure 3.3 shows that for $p_{SU} = 0.2$ the optimal ρ values are closer to 1. This is because now the dual cells are more congested and the SU network needs more temporal opportunities to balance its traffic and attain the highest capacity.

3.5 Conclusions

This chapter presented a hybrid secondary access method which combines the use of temporal opportunities with spatial opportunities. For the latter scheme we introduced the new concept of dual tessellation. The objective is enabling an operator to reuse the spectrum of a legacy cellular network of its own. The terminals of the newest network are secondary users for the legacy network. The operator can control the proportion of SUs using each access scheme by determining the probability ρ of using temporal opportunities. In terms of capacity for the SUs, the optimal ρ depends on the traffic intensity of the primary and the secondary networks. Therefore, the operator should monitor these intensities in order to determine the optimal ρ ,

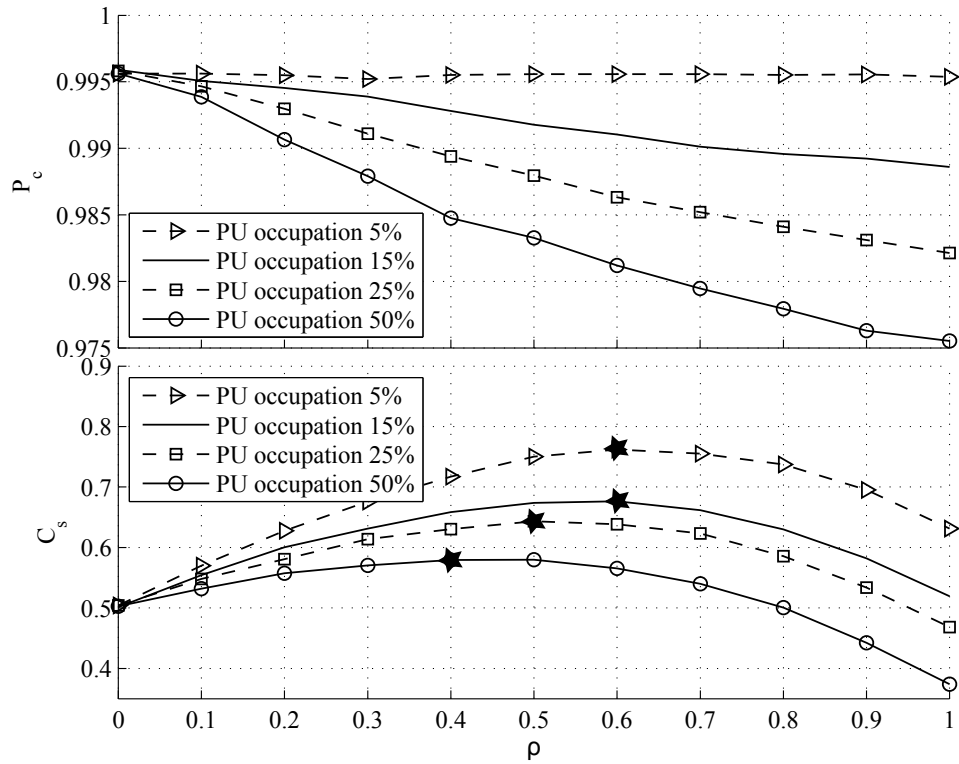


Figure 3.3: PU and SU performance versus ρ under different PU traffic intensities, for $p_{SU} = 0.2$. The stars indicate the optimum SU capacity for each PU occupation.

while assuring that the PU performance remains above a given threshold value. Because the optimal ρ is, in general, different from 0 and 1, the hybrid access provides higher secondary capacity than any of the two access methods separately.

Chapter 4

Stochastic Optimization Approach: The Unconstrained Case

4.1 Introduction

In chapter 3 we proposed a secondary hybrid access scheme in which the SUs can use temporal or spatial opportunities. To improve the secondary capacity the operator (the owner of primary and secondary networks) needs to achieve the optimum ρ parameter. In this chapter we propose an algorithm that dynamically learns the optimal parameters in a more general scenario.

Similar to the previous chapter, the cognitive pair (SUs) establish point-to-point connections among them in an ad-hoc fashion.

We propose a semi-decentralized secondary access scheme allowing each SU to access a set of primary frequency bands using either temporal or spatial spectrum holes (opportunities). By giving more access options to each SU, this approach can outperform previous, more limited, mechanisms. To fully exploit its potential, we describe an on-line algorithm that, with very small computational and signaling overhead, allows the system to learn the optimal SU access policy in terms of capacity.

The contribution of this chapter is a semi-distributed mechanism for opportunistic spectrum access in which *all the spectrum of the system can be made available* to each SU. The chapter 3 is substantially improved in the following aspects: 1) Each SU can still exploit spatial and temporal opportunities, but over a larger amount of bandwidth, resulting in higher SU capacity. 2) The system is evaluated in a more realistic setting considering irregular cell shapes. 3) And, the most important feature, *the system is capable of learning the optimal probability distribution over the frequency bands of the cellular network*. The learning algorithm applies the Response Surface Methodology (RSM) [12], which is a novel and promising approach to address interference management problems.

In the following section we describe the system. Section 4.3 formulates the design problem and Section 4.4 presents the RSM algorithm to solve it. Finally, Sections 4.5 and 4.6 present the numerical results and the conclusions of this work.

4.2 System description

The system considered comprises: a legacy cellular network (primary network), a secondary network establishing ad-hoc point-to-point links, and a secondary access controller (SAC) which monitors the system performance and broadcasts the operation parameters of the SU access strategy (with small signaling overhead, as we discuss in Section 4.4). The primary network contains base stations (PBSs) and primary users (PUs). Each PBS covers a certain geographical area (primary cell) and is assigned a frequency band different from its adjacent cells. We assume a frequency reuse scheme of 7 frequency bands (reuse factor 7), denoted by f_1, \dots, f_7 . Nevertheless, the proposed method can be applied to other reuse factors as well. Each frequency band is divided into $2N$ orthogonal channels (N downlink and N uplink channels). Secondary access is constrained to downlink channels. Time is divided into equal duration time-slots, which is usual in most cellular systems. The data transmitted over a single PU channel in a time-slot is referred to as *packet*.

The secondary network consists of pairs of secondary users (SUs) entering and leaving the system in an ad-hoc fashion. This network model can characterize femtocells, terminals acting as relays, or any short-range transmission using available spectral resources of the legacy cellular network. The SAC is associated to the network to which the SUs belong. In particular, we assume that the SUs are the users of a new generation cellular network. Because both networks (the new generation network and the legacy one) belong to the same operator, we consider that the SAC can retrieve some information from the legacy network.

The SUs can detect the power of the pilot tones of the neighboring PBSs. With this information (and possibly with the aid of the SAC) each SU can infer its position with respect to the surrounding cells and therefore be aware of the PBS power levels from each frequency band. Indeed, the SU does not need to estimate exactly these PBS power levels, it just needs to establish an ordering of the frequencies f_1, \dots, f_7 from lower to higher PBS power level. For a generic SU, let $\phi = (\phi_1, \dots, \phi_7)$ be the vector of frequencies ordered in increasing received power, which clearly depends on the location of the SU. Note that ϕ_7 corresponds, in general, to the frequency band of the primary cell where the SU is located.

Example. In Figure 4.1, any SU located in area A has $\phi_1 = f_1$ (similarly, any SU in area B has $\phi_1 = f_2$). But because each SU is closer to a different PBS, $\phi_7 = f_5$ for SU 1, and $\phi_7 = f_6$ for SU 2. These SUs have also different values of ϕ_2 and ϕ_4 .

When an SU transmits over any band ϕ_i , it may cause some interference to the PUs of the closest cells using this band (and the same channel within this band). According to the principles of frequency reuse in cellular networks, the average level of SU interference caused at PU receivers is proportional to the ordering index i of the selected band ϕ_i , i.e. a single SU transmission over ϕ_1 causes interference on the most distant cell, a transmission over ϕ_2 interferes on the second most distant cell and so forth. In our system, the classic strategy of occupying exclusively *spatial opportunities*, implies that each SU only tries to access over ϕ_1 . However, what really matters is the aggregate interference at the receivers. Note that, in accordance to the ad-hoc nature of the secondary network (small SU transmission range, low antenna heights, indoor locations

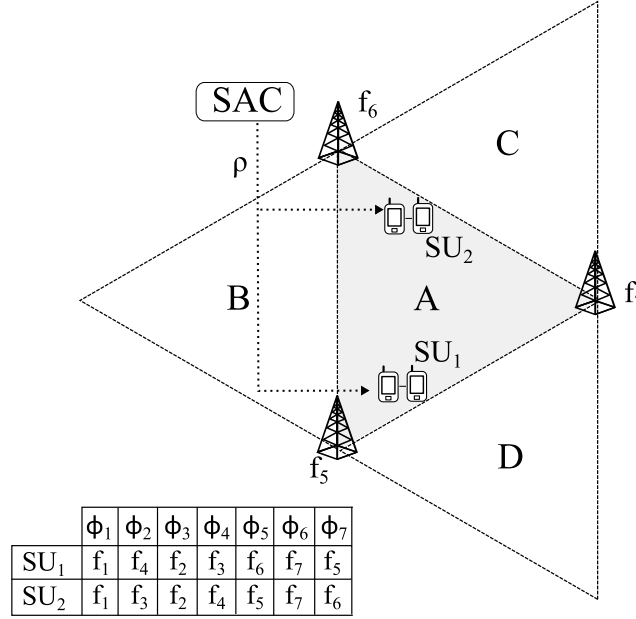


Figure 4.1: Example of the system with 2 SU pairs. Every SU in area A associates f_1 to ϕ_1 . The remaining f_j - ϕ_i associations for each SU depend on how close the SU is to areas B, C or D. The SAC broadcasts a vector of operation parameters ρ to the SUs.

sometimes) the PU receivers can still decode packets even some SUs select other bands different from ϕ_1 . The potential benefit of giving more frequency band options to the SUs is to decrease the inter-SU interference, increasing the capacity of the secondary network.

Besides, when an SU tries to access the band of a close PBS, i.e. a band associated to a higher interference power such as ϕ_7 , the SU can perform *PU activity detection* on the channels within the band [11]. This activity detection allows the SU to detect free channels before starting transmission, and to stop SU transmission when detecting overlap with PU transmissions. The closer the SU is to the PBS, the more reliable is the PU activity detection and therefore the less impact on PU communication. The free channels in ϕ_7 are identified as *temporal opportunities* in chapter 3.

As we showed in chapter 3 the typical strategies of using only spatial opportunities (ϕ_1 channels) or only temporal ones (ϕ_7 free channels) are not optimal, and an hybrid scheme combining both types of access increases the capacity of the system. The challenge was to find the optimal balance between the fraction of the SU population exploiting each type of spectrum opportunities. In this work we incorporate a learning strategy to address this issue, and we extend the hybrid access idea by allowing the SU to use 3 or more bands from its ϕ vector.

Now let us describe the proposed **secondary access scheme** over a spectrum comprising R frequency bands (R denotes the frequency reuse factor of the primary cellular network). Let us define the probability distribution $\rho = (\rho_1, \dots, \rho_R)$, where $0 \leq \rho_i \leq 1$ for $i = 1, \dots, R$, and $\sum_{i=1}^R \rho_i = 1$. Let \mathcal{P} denote the set of possible values of ρ . Before transmitting, each SU randomly selects one band, ϕ_i from its ϕ vector, according to the probability distribution ρ , i.e. $P(\text{select band } \phi_i) = \rho_i$. Once the SU has selected a particular band, ϕ_i , if the SU is capable of detecting enough PBS power in ϕ_i to perform PU activity detection, then the SU tries to access

over temporal opportunities, occupying only channels that are free of PU activity. Otherwise, the SU will access any channel with a sufficiently low SINR (considering also the interference from other SUs).

The value of ρ should be determined by the SAC, which broadcasts it to the SUs. The objective pursued in ρ computation is to maximize the system performance. In the envisioned scenario, the performance metric is the capacity achieved by the SUs, subject to a given constraint on the probability of correct packet reception at the PU receivers. Next section formalizes the problem in these terms. As we show in Section 4.4, the SAC aims to *learn* the optimal ρ^1 based on the performance measurements retrieved from the primary and the secondary devices.

Note that the outlined mechanism performs a semi-decentralized resource allocation. The ρ learning process is centralized at the SAC, while each SU decides autonomously which channel to occupy, based on ρ and its own spectrum sensing over the selected band. The signaling overhead consists of periodic broadcast messages from the SAC to the SUs *announcing* the updates of ρ , and one feedback packet from each terminal to the SAC after each session, containing the performance metric measured during the session.

4.3 Problem Formulation

In this section we define the performance metrics for both the PUs and SUs and formulate the problem that the SAC needs to solve to determine the ρ vector.

Let us consider a secondary network with a given traffic intensity characterized by its arrival rate per area unit, and a random transmission time. As stated above, the vector ρ determines how the SUs distribute themselves over the available spectrum and the proportion of SUs using PU activity detection. In consequence, the SINR at each PU or SU receiver depends on ρ . Let N_t^{SU} and N_t^{PU} denote the number of SUs and PUs in the system, respectively, at time-slot $t = 1, 2, \dots$. The SINR over time at an SU receiver $s \in \{1 \dots N_t^{SU}\}$, is a discrete time stochastic process induced by ρ , and denoted by $\Gamma_t^s(\rho)$. The expected normalized capacity per active SU pair is given by

$$C_s(\rho) = E \left\{ \lim_{T \rightarrow \infty} \frac{1}{T} \sum_{t=0}^T \sum_{s=1}^{N_t^{SU}} \frac{\log_2(1 + \Gamma_t^s(\rho))}{N_t^{SU} C_{\max}^S} \right\} \quad (4.1)$$

where C_{\max}^S is the maximum achievable SU capacity per Hertz. The expectation is taken over Γ_t^s and N_t^{SU} .² At a PU receiver, it is assumed that a data packet transmitted on time-slot t is correctly decoded if its SINR, Γ_t^{PU} , is greater than a given detection threshold, γ^{PU} . Then, the

¹It is advisable to divide the system into relatively homogeneous regions in terms of PBS density, traffic intensity and type of terrain, so that a suitable ρ can be found for each region.

²Note that the traffic intensity in a cellular communication network varies during a day, but if it is observed during a smaller time window, e.g. 1 hour, the traffic arrival process can be considered stationary, with constant intensity.

probability of correct detection at a PU is defined as

$$P_c(\rho) = E \left\{ \lim_{T \rightarrow \infty} \frac{1}{T} \sum_{t=0}^T \sum_{j=1}^{N_t^{PU}} \frac{\mathbb{I}_{\{\Gamma_t^j(\rho) > \gamma^{PU}\}}}{N_t^{PU}} \right\} \quad (4.2)$$

where Γ_t^j refers to the SINR process at the j -th active PU, and $\mathbb{I}_{\{z\}}$ is an indicator function which equals 1 if condition z holds, and equals 0 otherwise.

Therefore, the objective of the SAC is to find ρ solving the following problem

$$\begin{aligned} & \max_{\rho} C_s(\rho) \\ & \text{s.t.} \\ & P_c(\rho) \geq P_{c,\min} \\ & \rho \in \mathcal{P} \end{aligned} \quad (4.3)$$

where $P_{c,\min}$ denotes the minimum acceptable P_c .

Finding an optimal ρ is a challenging task because the (multiple) SINR stochastic processes capture the interaction of a random number of randomly located terminals with fading effects among each pair of them. Moreover, these processes and the decision vector ρ , take values from continuous spaces, and therefore conventional dynamic programming techniques result infeasible. The problem (4.3) is, in fact, a *stochastic optimization problem with stochastic constraints* [12]. As usual in this type of problems, the SAC has to dynamically *learn* an optimal ρ . One feasible way to address it is by means of Surface Response Methods (RSM) [13]. However, the inclusion of stochastic constraints introduces high complexity in the formulation. In the following section we develop the particular case in which $P_{c,\min}$ is sufficiently low for condition $P_c(\rho) \geq P_{c,\min}$ to hold at the optimal ρ (in numerical results, $P_c(\rho)$ at the optimal ρ is never less than 5% of the P_c obtained in absence of SU access). This allows us to remove the stochastic constraint regarding $P_c(\rho)$. In the next chapter we address this problem including the constraints in the RSM formulation.

4.4 Response Surface Method (RSM) Algorithm

4.4.1 Algorithm Formulation

The aim of the algorithm is the maximization of the expected value of the average capacity function (4.1) on a closed convex feasible domain $\mathcal{P} \subset \mathbb{R}^R$ for the input vector ρ , that is, to find a ρ approximately solving

$$\max_{\rho \in \mathcal{P}} C_s(\rho) \quad (4.4)$$

RSM allows us to find an approximate solution to this problem by successively estimating the gradient of the objective function and using these estimations in stochastic gradient ascent steps. At each one of these steps, numbered by $n = 1, 2, \dots$, the system generates one update of the

input vector $\rho_{(n)}$ according to the following expression

$$\rho_{(n+1)} = \rho_{(n)} + \alpha_{(n)} \hat{\nabla} C_s(\rho_{(n)}) \quad (4.5)$$

where $\hat{\nabla} C_s$ denotes the estimation of the gradient ∇C_s , and $\alpha_{(n)}$ is the step-size weighting factor. A standard condition for the selection of $\alpha_{(n)}$, assuring the convergence of $\rho_{(n)}$ [12], is $\sum_{n=1}^{\infty} \alpha_{(n)} = \infty$, $\sum_{n=1}^{\infty} \alpha_{(n)}^2 < \infty$.

Let us discuss the computation of $\hat{\nabla} C_s$. Given $\rho_{(n)}$ at step n , we consider a subdomain $\mathcal{S}_{(n)}$ of the feasible domain \mathcal{P} such that $\rho_{(n)} \in \mathcal{S}_{(n)} \subset \mathcal{P}$. Note that $\rho_{(n)}$ is the point at which the estimate $\hat{\nabla} C_s$ must be computed. Therefore, we need to estimate the objective function $C_s(\rho_{(n)})$ on $\mathcal{S}_{(n)}$, by taking samples $y^{(i)}, i = 1, \dots, p$, of the function. For this, we need a finite set of points $\rho_{(n,i)}, i = 1, \dots, p$, generally called *design points*, belonging to $\mathcal{S}_{(n)}$. These points are chosen by the decision maker (the SAC in our case), and can be, for example, random perturbations of $\rho_{(n)}$, falling within $\mathcal{S}_{(n)}$.

Let $t_{(n)}$ denote the time-slot in which the update $\rho_{(n)}$ is obtained. Given the set of p decision points, the SAC can obtain samples $y^{(i)}$ by this simple procedure:

1. Determine p sampling instants $t_{(n,i)} = t_{(n)} + iT$ for $i = 1 \dots p$, where T is a sufficiently long time period for measuring performance at the SUs.
2. At $t_{(n,i-1)}$ (where $t_{(n,0)} = t_{(n)}$), the SAC signals the design point $\rho_{(n,i)}$ to the SUs, for $i = 1 \dots p$.
3. At $t_{(n,i)}$, the SAC obtains the capacity samples from each active SU and averages them to obtain $y^{(i)}$.

Thus, the estimates can be expressed as

$$y^{(i)} = \frac{1}{T} \sum_{k=t_{(n,i-1)}}^{t_{(n,i)}} \sum_{s=1}^{N_k^{SU}} \frac{\log_2(1 + \Gamma_k^s(\rho_{(n,i)}))}{N_k^{SU} C_{\max}^S} \quad i = 1, 2, \dots, p, \quad (4.6)$$

Note that the stochastic ascent algorithm needs p periods of length T to upgrade $\rho_{(n+1)}$.

The objective function C_s is then approximated on $\mathcal{S}_{(n)}$ by a polynomial response surface model $\hat{C}_s(\rho) = \hat{C}_s(\rho|\beta_0, \beta_1 \dots \beta_R)$. The coefficients β_j , are determined by least squares estimation. Therefore, the RSM-gradient estimator $\hat{\nabla} C_s(\rho_{(n)})$ at $\rho_{(n)}$ is defined by the gradient (with respect to ρ)

$$\hat{\nabla} C_s(\rho_{(n)}) = \nabla \hat{C}_s(\rho_{(n)}). \quad (4.7)$$

Thus, C_s is estimated on $\mathcal{S}_{(n)}$ by the linear empirical model

$$\hat{C}_s(\rho_n) = \beta_0 + \beta_I^T(\rho - \rho_n) \quad (4.8)$$

where

$$\beta = (\beta_0, \beta_I^T)^T = (\beta_0, \beta_1, \dots, \beta_R)^T \quad (4.9)$$

is the $(R + 1)$ -vector of unknown coefficients of the linear model. Having samples $y^{(i)}$ of the function values $C_s(\rho_{(n,i)})$ at the design points $\rho_{(n,i)}, i = 1, \dots, p$, in $S_{(n)}$, we can obtain, by least squares, the following estimate $\hat{\beta}$ of β :

$$\hat{\beta} = (W^T W)^{-1} W^T y. \quad (4.10)$$

Here, the $p \times (R + 1)$ matrix W and the p dimensional vector y are defined by

$$W = \begin{pmatrix} 1 & \delta^{(1)} \\ 1 & \delta^{(2)} \\ \vdots & \vdots \\ 1 & \delta^{(p)} \end{pmatrix}, \quad y = \begin{pmatrix} y^{(1)} \\ y^{(2)} \\ \vdots \\ y^{(p)} \end{pmatrix} \quad (4.11)$$

with $\delta^{(i)} = \rho_{(n,i)} - \rho_{(n)}$, for $i = 1, 2, \dots, p$. Note that $(W^T W)$ in (4.10) is invertible whenever the columns of W are linearly independent, which can be easily guaranteed by a proper selection of the design points.

In case $C_s(\rho)$ is concave on \mathcal{P} , the RSM algorithm will approach the global optimum following the stochastic gradient ascent iterations (4.5). For the case of 2-dimensional ρ vectors, $C_s(\rho)$ was concave for the numerical simulations in the previous chapter. This property has also been observed for $R > 2$ dimensions in the scenarios considered in the following Section.

4.4.2 System Operation

The following steps summarize the **system operation**:

1. The SAC periodically updates the vector ρ and sends it to the SUs.
2. Each SU builds its own ϕ vector by scanning the PBS pilot tones on each frequency band. This vector only needs to be updated when the SU changes its location.
3. Before transmitting, an SU randomly selects one band, ϕ_i from its ϕ vector, according to the probability distribution ρ , i.e. $P(\text{select band } \phi_i) = \rho_i$.
4. If the SU is capable of detecting enough PBS power in ϕ_i to perform PU activity detection, then the SU tries to access over temporal opportunities, occupying only channels free of PU activity. Otherwise, the SU will access any channel with a sufficiently low SINR (considering also the interference from other SUs).
5. Periodically, the SAC retrieves information from both the primary and the secondary networks, particularly performance measures, which are taken into account to update vector ρ .

4.5 Numerical Results

4.5.1 Evaluation Framework

This subsection describes the Monte-Carlo methodology and the scenario used to evaluate C_s . There are some differences with respect to the scenario we proposed in the previous chapter. The primary network uses a 7-band frequency planning, as previously stated, with irregular shaped cells having an average radius $r = 700$ m. We consider pathloss and multipath fading. To compute the pathloss attenuation over distance, we use the same dual-slope model we proposed in the last chapter (section 3.4)

As we appoint in chapter 3, the critical distance d_c is notably smaller for SU transmission than for PBS transmissions, because the PBSs are located at high outdoor locations while SUs are, in general, located either indoors or at ground level. All the signals are assumed to experience Rayleigh fading.

The area used to generate random terminal locations is a $4.2 \text{ Km} \times 4.8 \text{ Km}$ rectangle. We focus on the downlink channels of one frequency band. We consider an scenario in which the primary traffic intensity is low $0.16 \text{ Erlangs/Km}^2$, so that the average occupation of the spectrum by the primary terminals is only 5%. In contrast, the SU traffic intensity, $27.5 \text{ Erlangs/Km}^2$, is high in comparison. In this case, the SU capacity is mostly determined by the inter-SU interference and the RSM algorithm is essentially performing *interference management* in the SU network. We also discuss the effect of higher PU spectrum occupation and a different SU traffic intensity. According to the ad-hoc nature of the secondary network, the average SU link distance considered is 90 m. Table 4.1 summarizes the simulation parameters considered.

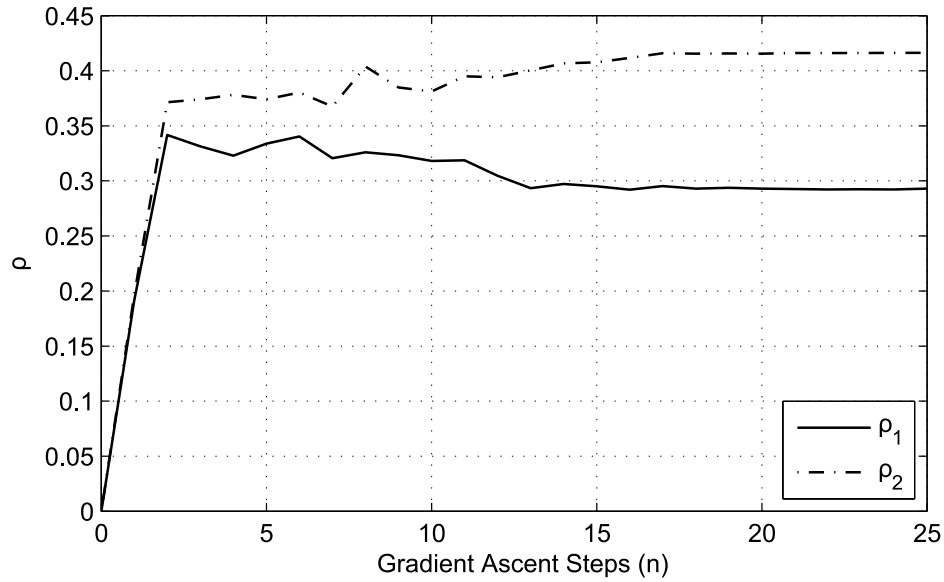
4.5.2 Convergence and Usage of the Frequency Bands

Let us consider the case of 3-dimensional ρ vectors, $R = 3$. In this case, the ρ vector of a particular SU is $\rho = (\rho_1, \rho_2, \rho_3)$, being ρ_3 the probability of trying to access the band ϕ_7 of the primary cell where the SU is in, and ρ_1 and ρ_2 the probabilities of accessing ϕ_1 and ϕ_2 , the bands where the SU receives less PBS power. The SU can only perform PU activity detection on ϕ_7 channels, while the channels of the other bands are considered spatial opportunities. Fig. 4.2 shows the values of ρ_1 and ρ_2 (ρ_3 is simply $1 - \rho_1 - \rho_2$) over consecutive update steps $n = 1, 2, \dots$. The initial vector is $\rho_0 = (0, 0, 1)$. Although ρ_0 is a rather poor initial guess, we see that the RSM algorithm stabilizes after 20 iterations. The final value is $\rho = (0.29, 0.42, 0.29)$. Fig. 4.3 shows the estimated value of C_s as a function of ρ_1 and ρ_2 . Consistently with the result obtained by RSM, the maximum values of C_s lie on the line $\rho_1 + \rho_2 = 0.7$.

Let us now consider the results for $R = 5$. The probability ρ_5 is now associated to ϕ_7 , allowing PU activity detection, while $\rho_1 \dots \rho_4$ are associated to $\phi_1 \dots \phi_4$, where PU activity detection is assumed to be unfeasible. The initial ρ vector is $(0, 0, 0, 0, 1)$. Figure 4.4 shows that, in this case, the convergence of RSM is as fast as with $R = 3$. Note that, as in the case of $R = 3$, the algorithm is not assigning ρ_1 the highest probability. The reason is that the algorithm aims to

| Parameter | Assigned value |
|---|------------------|
| Primary transmitters | |
| number of downlink channels, N | 5 |
| cell radius, r | 700 m |
| average received power at PU | -78 dBm |
| SINR detection threshold at PU, γ^{PU} | -17 dB |
| baseline noise at PU ($N_0 + I_{PU}$) | -110 dBm |
| Secondary transmitters | |
| average SU Tx power per channel | 0.5 W |
| SU link distance | 90 m |
| probability of PU activity detection | 0.9 |
| probability of overlap detection | 0.8 |
| Propagation parameters | |
| pathloss exponents, γ_1, γ_2 | 2.4, 4.2 |
| propagation factor K | 46.7 dB |
| critical distance for PBS transmission | $1.2r$ m |
| critical distance for SU transmission | 100 m |
| RSM parameters | |
| dimensions of ρ, R | $1 \dots 5$ |
| measuring period T (in time-slots) | 300 |
| number of samples per step p | $3(2^{R-1} + 1)$ |

Table 4.1: Parameter setting of the reference scenario used in numerical evaluations

Figure 4.2: Consecutive RSM updates of ρ_1 and ρ_2 .

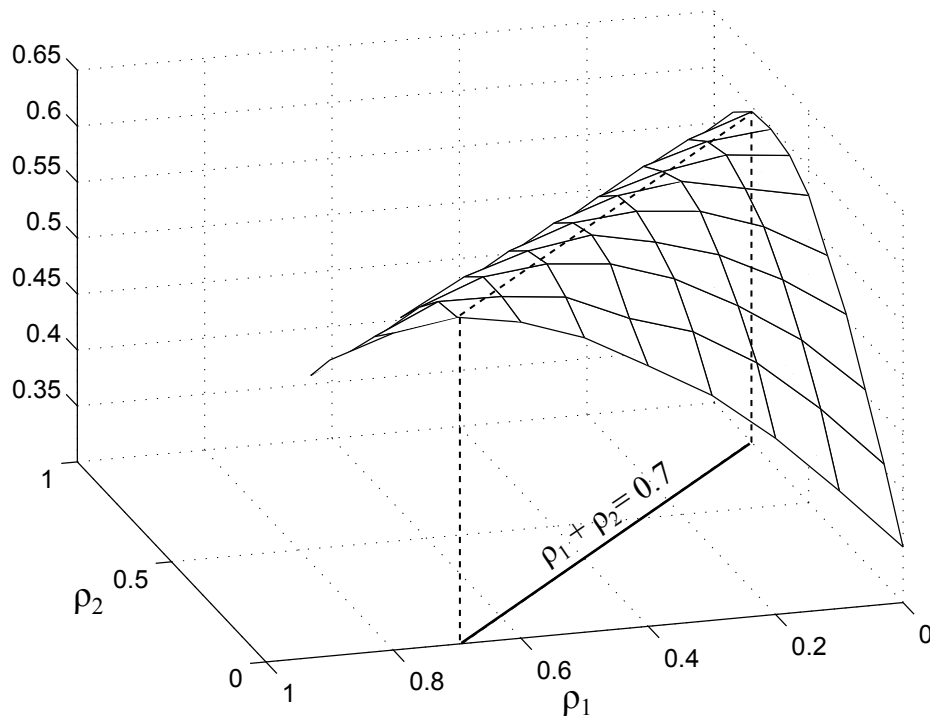
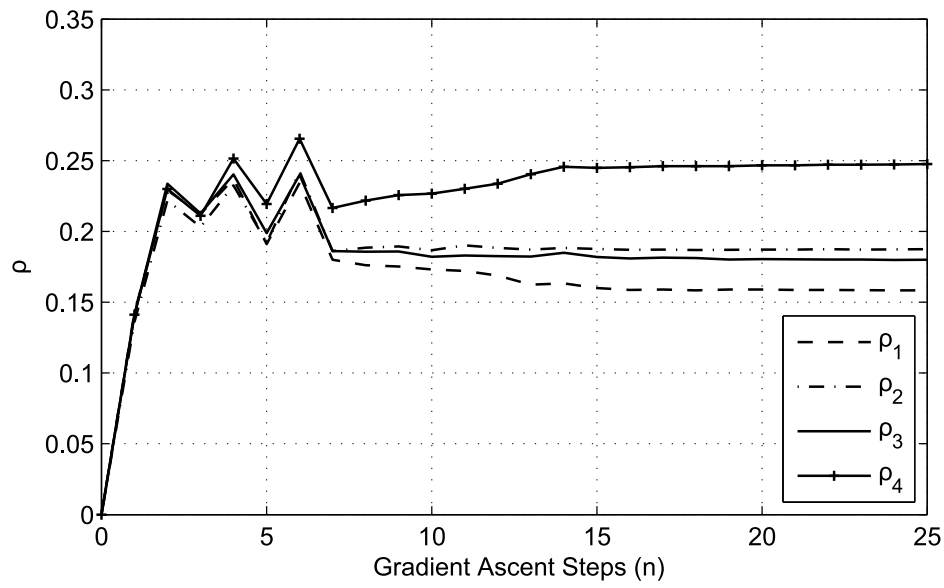
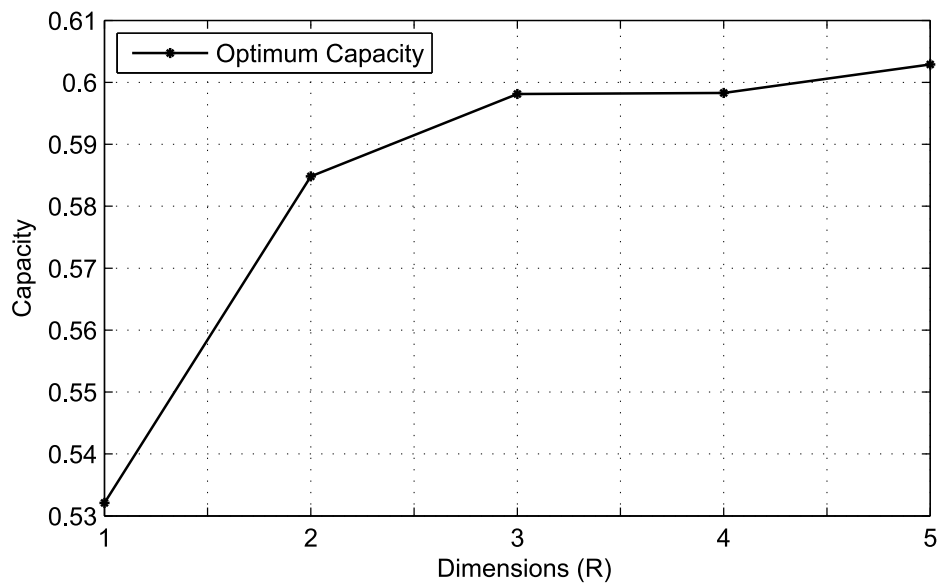


Figure 4.3: Estimation of C_s over ρ_1 and ρ_2 .

minimize inter SU interference by separating the SU transmitters using the same band. Recall that in Fig. 4.1 all the SUs in triangular region A shared the same ϕ_1 but had different values for ϕ_2 . The aggregated probability of using spatial opportunities is $\sum_{i=1}^4 \rho_i = 0.77$, which is higher than in the $R = 3$ case. This result confirms the idea that, the more spectrum is available to each SU, the more spectrum the SU exploits. Having more spectrum options per SU (higher R) also allows the SU network to achieve a higher capacity, as illustrated by Fig. 4.5.

4.5.3 Effect of the Traffic Intensity

Fig. 4.6 shows the average SU capacity attained by the RSM algorithm with $R = 2$, versus the average spectrum usage by the PUs, for different SU traffic intensities. As expected, the more spectrum occupied by PU traffic, the smaller the achieved capacity. Similarly, more SU traffic implies less SU capacity. The reason of the reduction on the maximum achieved capacity is the increment of the aggregate interference power at the SU receivers, from both the PBSs and other SU pairs. Compared to the typical approach of exploiting only temporal opportunities, the benefit of using RSM is noticeable for every traffic situation. In all cases, the reduction of the probability of correct detection at the PU receivers (P_c) was less than 5%.

Figure 4.4: Consecutive RSM updates of $\rho_1 \dots \rho_4$.Figure 4.5: Maximum SU capacity obtained with RSM versus the number of dimensions of ρ , R .

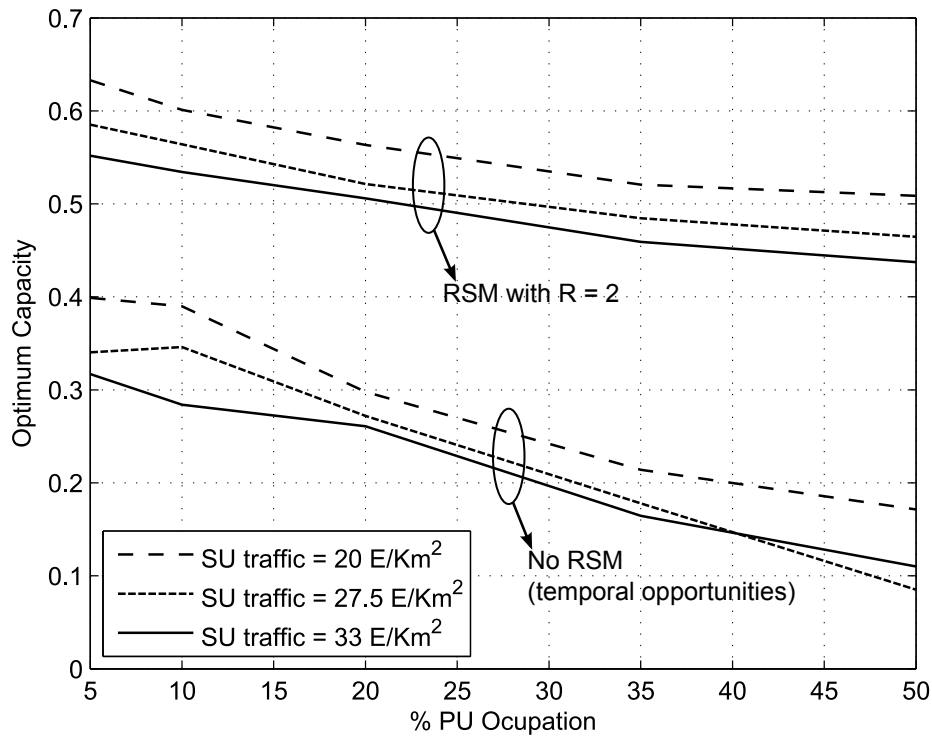


Figure 4.6: Maximum SU capacity obtained with RSM under different traffic intensities. For comparison, the figure also shows the capacity for a SU network exploiting only temporal opportunities (no RSM).

4.6 Conclusion

Motivated by the problem of spectrum reuse in cellular networks, in this chapter we presented a semi-distributed mechanism allowing the secondary network to learn the most efficient spectrum access strategy. This mechanism exploits both spatial and temporal opportunities, and is especially effective for interference management in highly dense secondary networks. The learning approach is based on response surface methodology (RSM) which, according to the numerical results, improves notably the system capacity compared to usual strategies, and shows a fast convergence rate even when it is poorly initialized. Because of that, the system can adapt its control vector ρ to variations on the traffic intensity or user distribution. Surprisingly, the use of RSM on this framework had not been reported on previous works. The next chapter is focused on incorporating performance constraints for the primary network in the RSM formulation.

Chapter 5

Stochastic Constraints for Primary Transmission Protection

5.1 Introduction

In the previous chapter we proposed an algorithm that dynamically learns the optimal parameters in a general scenario where a secondary user can use all the frequencies available. In addition, we proposed a semi-decentralized secondary access scheme that allows each SU to access to the frequency bands using either temporal or spatial spectrum holes (opportunities).

In this chapter, we reformulate the algorithm adding stochastic restrictions that allows the system to find the optimum parameters and explore new solutions always satisfying the minimum requirements of the primary system.

Besides, we propose a new scenario where the primary and secondary traffic intensities change throughout the day. In this scenario, we evaluate two types of users (corresponding to primary and secondary users) with different traffic patterns.

5.2 System description

In this chapter, the system model is similar to the model we propose in chapter 4, (section 4.2) but there are some differences. We assume a frequency reuse scheme with reuse factor equals to 7. The frequency bands are denoted by f_1, \dots, f_7 . Each SU computes its frequency vector $\phi = (\phi_1, \dots, \phi_7)$ ordered in increasing received power. This vector is associated with the SU location. Therefore, an SU only needs to recalculate the ϕ vector when changing its position.

In this scenario, we consider that the SUs which use the frequencies ϕ_1, \dots, ϕ_5 will perform access over spatial opportunities (section 3.2.1). The SUs using the remaining frequencies (ϕ_6 and ϕ_7) will access over temporal opportunities because this SUs are near enough to the PBS to perform PU activity detection.

Although ϕ_6 and ϕ_7 perform access over spatial opportunities, the effects of this two frequencies

at PU receivers are not the same. A SU using ϕ_6 causes less average interference. Nevertheless, the probability of overlapping transmissions between a primary and a secondary transmitter is higher because its detection probability decreases, that is, the more distance to PBS the lower detection accuracy.

In [14] the expression of probability detection is derived:

$$p_d = \frac{1}{\gamma} \int_0^{\infty} Q_{\lfloor sW \rfloor}(\sqrt{2\gamma}, \sqrt{\theta}) \exp(-\frac{\gamma}{\bar{\gamma}}) d\gamma \quad (5.1)$$

where $Q(., .)$ is the generalized Marcum Q-function, $\bar{\gamma}$ is the mean signal-to-noise ratio (SNR) observed by the SU energy detector, γ is the instantaneous SNR observed by the SU, θ is the PU signal detection threshold in dB, s is the scanning length in μs and W is the channel bandwidth in Hz. Equation 5.1 gives the probability of signal detection in the presence of Gaussian noise only averaged over the fading statistics. This equation has a closed-form solution given by

$$p_d = e^{-\frac{\theta}{2}} \left\{ \sum_{h=0}^{\lfloor sW \rfloor - 2} \frac{\theta^h}{h! 2^h} + \left(\frac{1 + \bar{\gamma}}{\bar{\gamma}} \right)^{\lfloor sW \rfloor - 1} \times \left[e^{\frac{\theta \bar{\gamma}}{2 + 2\bar{\gamma}}} - \sum_{h=0}^{\lfloor sW \rfloor - 2} \frac{(\theta \bar{\gamma})^h}{h! 2 + 2\bar{\gamma}^h} \right] \right\} \quad (5.2)$$

5.3 Response Surface Method (RSM) Algorithm with Stochastic Constraints

5.3.1 Algorithm Formulation

The aim of the algorithm is the maximization of the expected value of the average capacity function (4.1) over the control vector ρ on a closed convex feasible domain $\mathcal{P} \subset \mathbb{R}^R$ subject to P_c is above the minimum required value $P_{c,min}$. That is, the algorithm must find a ρ solving

$$\begin{aligned} & \max_{\rho} C_s(\rho) \\ & \text{s.t.} \\ & P_c(\rho) \geq P_{c,min} \\ & 0 \leq \rho_i \leq 1 \\ & \text{for } i = 1, \dots, R \end{aligned} \quad (5.3)$$

We will refer to C_s as F_0 and P_c as F_1 . The first stage of the algorithm requires first-order polynomials approximations of the functions F_i for $i = 0, 1$ augmented with noise:

$$G_i(\rho) = \tilde{\rho}' \beta_i + \varepsilon_i(\rho) \quad i = 0, 1 \quad (5.4)$$

where $\tilde{\rho} = (1, \rho')'$ and $\beta_i \in \mathbb{R}^{R+1}$ denotes the vector of $R+1$ polynomial coefficients (including the intercept), and ε_i is the additive noise. When the white-noise assumption is satisfied, ordinary least squares (OLS) gives the best linear unbiased estimator (BLUE) of β_i . Here ‘best’

means giving the lowest variance of the estimate as compared to other unbiased linear estimators. The assumption of the white-noise is discussed in [15].

Let us discuss the computation of first-order polynomial approximation. Given $\rho_{(n)}$ at step n , we consider a subdomain $\mathcal{S}_{(n)}$ of the feasible domain \mathcal{P} such that $\rho_{(n)} \in \mathcal{S}_{(n)} \subset \mathcal{P}$. Note that $\rho_{(n)}$ is the point at which the linear approximation must be computed. Therefore, we need to estimate the objective function $C_s(\rho_{(n)})$ on $\mathcal{S}_{(n)}$, by taking samples $y^{(i)}, i = 1, \dots, p$, of the function. For this, we need a finite set of points $\rho_{(n,i)}, i = 1, \dots, p$, generally called *design points*, belonging to $\mathcal{S}_{(n)}$. These points are chosen by the decision maker (the SAC in our case), and can be, for example, random perturbations of $\rho_{(n)}$, falling within $\mathcal{S}_{(n)}$.

The objective function C_s is then approximated on $\mathcal{S}_{(n)}$ by a first-order polynomial response surface model $\hat{C}_s(\rho) = \hat{C}_s(\rho|\beta_0, \beta_1 \dots \beta_R)$. The coefficients β_j , are determined by least squares estimation. Therefore, C_s is estimated on $\mathcal{S}_{(n)}$ by the linear empirical model

$$\hat{C}_s(\rho_n) = \beta_0 + \beta_I^T(\rho - \rho_n) \quad (5.5)$$

where

$$\beta = (\beta_0, \beta_I^T)^T = (\beta_0, \beta_1, \dots, \beta_R)^T \quad (5.6)$$

is the $(R+1)$ -vector of unknown coefficients of the linear model. Having samples $y^{(i)}$ of the function values $C_s(\rho_{(n,i)})$ at the design points $\rho_{(n,i)}, i = 1, \dots, p$, in $\mathcal{S}_{(n)}$, we can obtain, by least squares, the following estimate $\hat{\beta}$ of β :

$$\hat{\beta} = (W^T W)^{-1} W^T y. \quad (5.7)$$

Here, the $p \times (R+1)$ matrix W and the p dimensional vector y are defined by

$$W = \begin{pmatrix} 1 & \delta^{(1)} \\ 1 & \delta^{(2)} \\ \vdots & \vdots \\ 1 & \delta^{(p)} \end{pmatrix}, \quad y = \begin{pmatrix} y^{(1)} \\ y^{(2)} \\ \vdots \\ y^{(p)} \end{pmatrix} \quad (5.8)$$

with $\delta^{(i)} = \rho_{(n,i)} - \rho_{(n)}$, for $i = 1, 2, \dots, p$. Note that $(W^T W)$ in (5.7) is invertible whenever the columns of W are linearly independent, which can be easily guaranteed by a proper selection of the design points.

After the β_i are estimated, our problem in (4.3) is locally approximated by

$$\begin{aligned} & \max_{\rho} \hat{\beta}_{0,-0}^T \rho \\ & \text{s.t.} \\ & \hat{\beta}_{1,-0}^T \rho \geq \underline{P_{c,\min}} \\ & 0 \leq \rho_i \leq 1 \\ & \text{for } i = 1, \dots, R \end{aligned} \quad (5.9)$$

where $\hat{\beta}_{i,-0}^T$ denotes the OLS estimate excluding the intercept $\hat{\beta}_{i,0}^T$, and $\underline{P}_{c,\min} = P_{c,\min} - \hat{\beta}_{1,0}^T$. In (5.9), we eliminate the intercept term ($\hat{\beta}_{0,0}$) from the objective function because we use only the gradient of the objective.

After reformulating the problem in terms of locally approximation, we derive an estimated search direction for the problem in (4.3). We introduce the slack vectors s , r and v :

$$\begin{aligned} & \max_{\rho} \hat{\beta}_{0,-0}^T \rho \\ & \text{s.t.} \\ & \hat{\beta}_{1,-0}^T \rho - s = \underline{P}_{c,\min} \\ & \rho + r = 1 \\ & \rho - v = 0 \\ & s \in \mathbb{R}, r, v \in \mathbb{R}^R \end{aligned} \tag{5.10}$$

Our intention is not to solve the linear programming problem in (5.10). Instead, we use the local approximation in (5.10) to derive a novel search direction using standard tools from interior point methods ([16], [17]).

$$d = (\hat{\beta}_{1,-0} s^{-2} \hat{\beta}_{1,-0}^T + \hat{R}^{-2} + \hat{V}^{-2})^{-1} \hat{\beta}_{0,-0} \tag{5.11}$$

where \hat{R} and \hat{V} are diagonal matrices whose diagonal elements are the current estimated slack vectors \hat{r} and $\hat{v} > 0$ respectively. The matrix within the parentheses of (5.11) is invertible, because $\hat{\beta}_{1,-0} s^{-2} \hat{\beta}_{1,-0}^T$ is positive semi-definite, and \hat{R}^{-2} and \hat{V}^{-2} are positive definite. The positive definiteness holds because each iterate is strictly feasible, and hence, each iterate lies in the interior of the feasible region. The last factor in (5.11), $\hat{\beta}_{0,-0}$, is the estimated steepest-ascent direction.

5.3.2 Algorithm Operation

The novelty of this algorithm is the computation of a search direction that takes into account the stochastic restrictions.

The part within parentheses of equation (5.11) modifies the steepest-ascent direction ($\hat{\beta}_{0,-0}$) according to the restrictions formulated in (5.3). Hence, the first part within parentheses of equation (5.11) ($\hat{\beta}_{1,-0} s^{-2} \hat{\beta}_{1,-0}^T$) refers to P_c restriction. The other two terms within parentheses of equation (5.11) ($\hat{R}^{-2} + \hat{V}^{-2}$) refers to the ρ_i range restriction and it takes into consideration that $0 \leq \rho_i \leq 1$ for $i = 1, \dots, R$.

Hence, as the value of a slack variable decreases (so the corresponding constraint gets tighter), the search direction deviates more from the steepest descent direction. Then, the proposed search direction avoids hitting the boundary of restrictions.

On the other hand, note that the ρ vector is a discrete probability distribution and therefore it must satisfy two conditions: the restriction of $0 \leq \rho_i \leq 1$ for $i = 1, \dots, R$ is satisfied in the formulation of the optimization problem (5.3), but ρ has to satisfy $\sum_{i=1}^R \rho_i = 1$ as well. For this

purpose we use a heuristic to scale the vector if necessary.

In practice, we optimize a $(R - 1)$ -dimensional vector $(\rho_1 \dots \rho_{R-1})$ and we calculate ρ_R as $1 - \sum_{i=1}^{R-1} \rho_i$. Therefore, we have to assure that $\sum_{i=1}^{R-1} \rho_i \leq 1$ at each iteration. In every iteration where that condition does not hold, we scale the $R - 1$ -dimensional ρ vector as follows: $\rho_i = \frac{\rho_i}{\sum_{i=1}^{R-1} \rho_i}$ for $i = 1, \dots, R - 1$.

5.3.3 Sampling and Update of the ρ Vector

Let $t_{(n)}$ denote the time-slot in which the update $\rho_{(n)}$ is obtained. Given the set of p decision points, the SAC can obtain samples $y^{(i)}$ by this simple procedure:

1. Determine p sampling instants $t_{(n,i)} = t_{(n)} + iT$ for $i = 1 \dots p$, where T is a sufficiently long time period for measuring performance at the SUs.
2. At $t_{(n,i-1)}$ (where $t_{(n,0)} = t_{(n)}$), the SAC signals the design point $\rho_{(n,i)}$ to the SUs, for $i = 1 \dots p$.
3. At $t_{(n,i)}$, the SAC obtains the capacity samples from each active SU and averages them to obtain $y^{(i)}$.

Thus, the estimates can be expressed as

$$y^{(i)} = \frac{1}{T} \sum_{k=t_{(n,i-1)}}^{t_{(n,i)}} \sum_{s=1}^{N_k^{SU}} \frac{\log_2 (1 + \Gamma_k^s(\rho_{(n,i)}))}{N_k^{SU} C_{\max}^S} \quad i = 1, 2, \dots, p \quad (5.12)$$

Note that the stochastic ascent algorithm needs p periods of length T to upgrade $\rho_{(n+1)}$.

5.4 Daily Traffic Application

In this section we evaluate the algorithm in a scenario where we consider two daily traffic patterns belonging to two different kind of users. This scenario simulates the operation of a real cellular network where the traffic intensities change throughout the day. The traffic pattern also changes depending on the type of user (voice, mobile data...).

We consider two types of traffic [18]. The primary traffic which belongs to the legacy network performs a classic telephone traffic pattern. On the other hand, the secondary network performs a data traffic pattern. Consequently, we have the superposition of two different traffic patterns which implies that the algorithm has to operate with very different primary and secondary traffic values.

Let us discuss the operation of the system. Since the primary and secondary traffic values change throughout the day, the results obtained by the algorithm will change a lot and the algorithm will never reach a stationary state. For this reason we divide the day into stages (time slots) and we consider that the traffic is constant within these stages. Thus, we run the algorithm

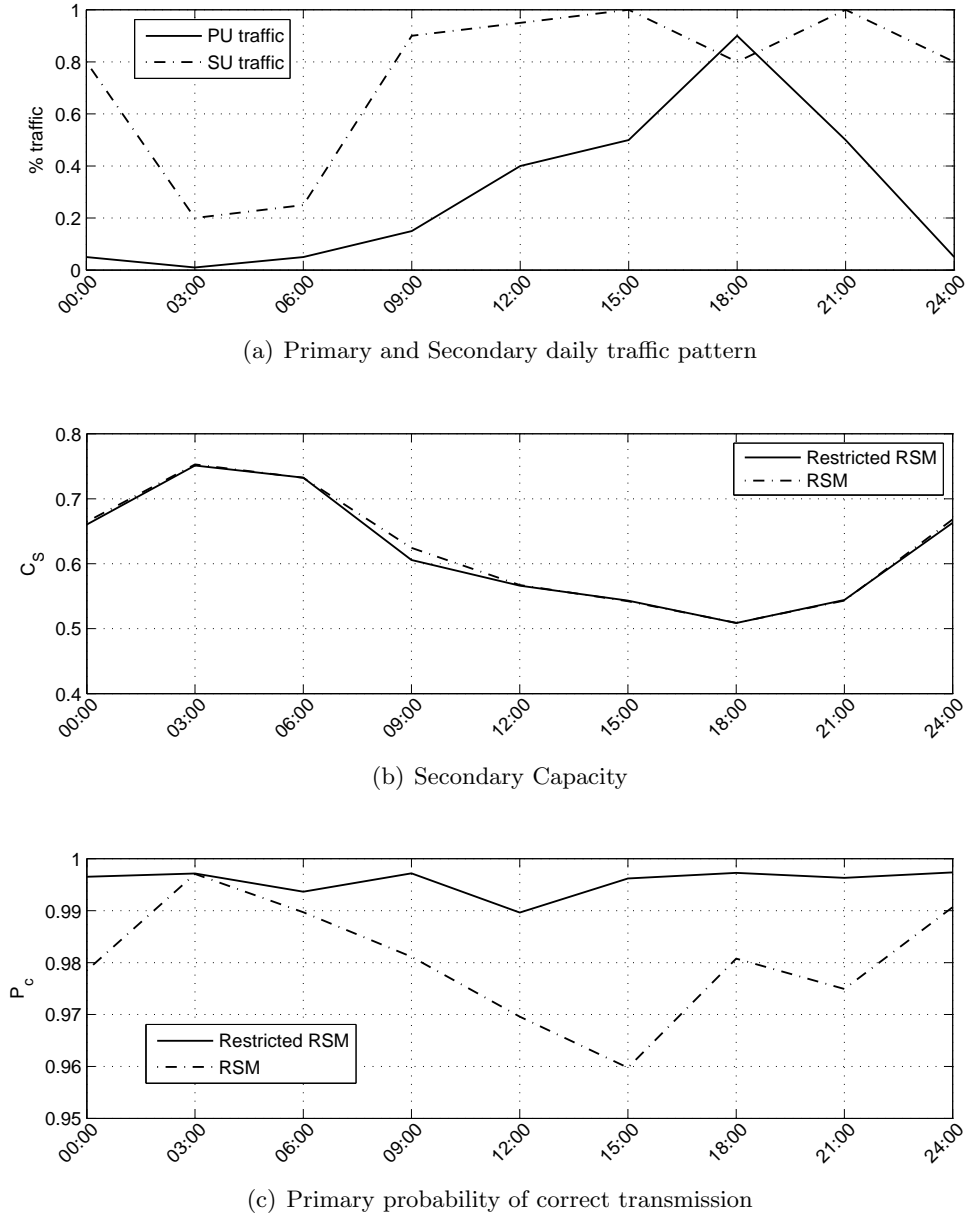


Figure 5.1: Evaluation of the algorithm in a scenario where we consider stationary traffic patterns.

with different parameters in each stage and, exploiting the fact that the traffic pattern repeats on a daily basis [18], we save the parameters until the same stage at next day. For instance, we run the algorithm in stage 1. At the end of this stage the algorithm save the ρ vector obtained and load the ρ vector of stage 2 (which was saved at the end of stage 2 the day before). Next day, at the beginning of stage 1 the vector which was saved the day before is loaded. Since the traffic is substantially similar to the traffic of the day before at this stage, the algorithm is really close to the optimum which is reached very quickly.

We have to consider the especial case of weekends where the traffic is lower. These two days are optimized separately of the rest of the week.

Figure 5.1(a) shows the traffic values of the two type of users throughout the day. Figure

5.1(b) shows that a lower PU traffic allows higher SU capacity, and a lower SU traffic increases the SU capacity as well. Figure 5.1(c) shows the quality of service for PUs, given by the P_c measured on each period.

Figure 5.1 also shows the different results obtained using RSM and Restricted RSM. Both algorithms get different ρ vectors with same capacity which means that the system has several local optima. Note that the Restricted RSM achieves a better local optima in terms of PU performance, that is, Restricted RSM achieves a solution with the same SU capacity but less harmful to primary users.

5.5 Conclusion

In this chapter we applied the response surface methodology (RSM) algorithm with stochastic restrictions to a scenario modeling the operation of a real cellular network where the traffic intensities change throughout the day.

The new formulation of the stochastic restrictions allows the algorithm to find the optimal configuration of the system always satisfying the minimum requirements of the primary system. We proposed a system operation based on dividing each day in stages which the traffic intensity can be considered stationary.

Chapter 6

Conclusion

Motivated by the problem of spectrum reuse in cellular networks where the frequency bands of the legacy networks become gradually underused, we present a novel semi-decentralized scheme which allows secondary users to access to all frequency bands combining the use of temporal opportunities with spatial opportunities. Hence, the operator is allowed to reuse the spectrum of its own legacy cellular network. The terminals of the newest network are secondary users for the legacy network.

The operator controls the proportion of SUs using each frequency band available and therefore, the proportion of SUs using each access scheme by determining the ρ probability vector. This access scheme is applicable to any cellular network reuse factor and all frequency bands are available for each SU. The type of access depends on the positions and the frequency band chosen by the SU. If an SU chooses a frequency band whose PBS is near enough to perform PU activity detection, this SU will access over temporal opportunities. Otherwise the SU will access over spatial opportunities.

An arbitrary value of ρ vector can increase the SU capacity but can also decrease the PU performance. Numerical results show that using this semi-decentralized scheme, the SU capacity can be increased holding the PU performance above of a minimum desired value.

In order to learn the optimal value of ρ we use a stochastic optimization algorithm called response surface methodology (RSM). According to the numerical results, this algorithm improves the system capacity and shows a fast convergence rate. Because of that, the system can adapt its control vector ρ to variations on the traffic intensity or user distribution.

We reformulate the optimization algorithm in order to assure that the PU performance remains above a given threshold value. The response surface algorithm with stochastic restrictions operate similarly to conventional RSM but taking into account the restriction of PU performance. Thus, it is equivalent to incorporating a security measure to protect the primary users while allowing the secondary users to explore new solutions in order to improve its capacity.

Finally, we evaluate the algorithm in a scenario where the traffic intensities change throughout the day. We evaluate two daily traffic patterns belonging to two different kind of users (primary and secondary). In order to assure the fast convergence of the algorithm, we divide each day into

stages where the traffic process can be considered stationary. Since the traffic follows a periodic pattern in a daily basis, the parameters can be saved at the end of each stage and loaded at the beginning of the same stage at the next day. Hence, the loaded parameters are very close of the optimum parameters and therefore, the optimum is reached quickly.

Bibliography

- [1] Alcaraz, J. J., Ayala-Romero, J. A., Lopez-Martinez, M., and Vales-Alonso, J., “Combining dual tessellation and temporal opportunities for spectrum reuse in cellular systems” , In *Wireless Communications Systems (ISWCS), 2014 11th International Symposium on.*, IEEE, 2014. p. 486-490.
- [2] J. J. Alcaraz, J. A. Ayala-Romero, M. Lopez-Martinez, J. Vales-Alonso, “Response Surface Methodology for Efficient Spectrum Reuse in Cellular Networks”, Accepted to *Communications (ICC), 2015 IEEE International Conference on.* IEEE, 2015
- [3] Mhiri, F., Sethom, K., and Bouallegue, R, *A survey on interference management techniques in femtocell self-organizing networks*, Journal of Network and Computer Applications, 2013, vol. 36, no 1, p. 58-65
- [4] D. Tuan, B.L. Mark, “Joint spatial-temporal spectrum sensing for cognitive radio networks” , *IEEE Transactions on Vehicular Technology*, vol.59, no.7, pp.3480,3490, Sept. 2010
- [5] Q. Wu et.al., “Spatial-Temporal Opportunity Detection for Spectrum-Heterogeneous Cognitive Radio Networks: Two-Dimensional Sensing,” *IEEE Trans. on Wireless Commun.*, vol.12, no.2, pp.516-526, Feb. 2013.
- [6] D. Guoru, et.al., “Joint exploration and exploitation of spatial-temporal spectrum hole for cognitive vehicle radios,” *2011 IEEE International Conference on Signal Processing, Communications and Computing (ICSPCC)*, pp.1-4, Sep. 2011.
- [7] M. G. Khoshkholgh, K. Navaie, and H. Yanikomeroglu, “Access strategies for spectrum sharing in fading environment: overlay, underlay and mixed,” *IEEE Trans. Mobile Comput.*, vol. 9, no. 12, pp. 1780-1793, Dec. 2010.
- [8] E.G. Larsson, M. Skoglund, “Cognitive radio in a frequency-planned environment: some basic limits,” *IEEE Transactions on Wireless Communications*, vol.7, no.12, pp.4800-06, Dec. 2008.
- [9] E. Axell, E.G. Larsson, D. Danev, “Capacity considerations for uncoordinated communication in geographical spectrum holes,” *Physical Communication*, vol. 2, no.1, pp- 3-9, Mar. 2009.
- [10] A. Goldsmith, *Wireless Communications*, Cambridge University Press, 2005.

- [11] E. Biglieri et.al., *Principles of Cognitive Radio*, Cambridge University Press, 2013.
- [12] K. Marti, *Stochastic Optimization Methods*, Springer-Verlag, Berlin-Heidelberg, 2008.
- [13] E. Angün et.al., *Response surface methodology with stochastic constraints for expensive simulation*, Journal of the Operational Research Society, 60 (6) (2009), pp. 735-746.
- [14] P. Pawelczak, et. al., *Performance analysis of multichannel medium access control algorithms for opportunistic spectrum access*, IEEE Trans. Veh. Technol., vol. 58, no. 6, pp. 3014-3031, July 2009.
- [15] Kleijnen, Jack PC., *Statistical tools for simulation practitioners*, Marcel Dekker, Inc., 1986.
- [16] Barnes, Earl R, *A variation on Karmarkar's algorithm for solving linear programming problems*, Mathematical programming 36.3 (1986): 174-182.
- [17] Angun, M. E, *Black box simulation optimization: generalized response surface methodology*, No. 2548e953-54ce-44e2-8c5b-7e4e2ac23afe. School of Economics and Management, 2004.
- [18] Kylesbech Larsen, K., *Capacity planning in mobile data networks experiencing exponential growth in demand*, Informa's 3G, HSPA & LTE Optimization Conference, 17th April 2012, Prague, Czech Republic.